



Regional brain morphology predicts pain relief in trigeminal neuralgia

Peter Shih-Ping Hung^{a,b}, Alborz Noorani^{a,b}, Jia Y. Zhang^c, Sarasa Tohyama^{a,b},
Normand Laperriere^d, Karen D. Davis^{a,b,e}, David J. Mikulis^{b,f}, Frank Rudzicz^{g,h,i},
Mojgan Hodaie^{a,b,e,j,*}

^a Division of Brain, Imaging & Behaviour, Krembil Brain Institute, Toronto Western Hospital, University Health Network, Toronto, Ontario, Canada

^b Institute of Medical Science, Faculty of Medicine, University of Toronto, Toronto, Ontario, Canada

^c Schulich School of Medicine & Dentistry, Western University, London, Ontario, Canada

^d Department of Radiation Oncology, University of Toronto, Toronto, Ontario, Canada

^e Department of Surgery, Faculty of Medicine, University of Toronto, Toronto, Ontario, Canada

^f Division of Neuroradiology, Joint Department of Medical Imaging, University Health Network, Toronto Western Hospital, Toronto, Ontario, Canada

^g Department of Computer Science, University of Toronto, Toronto, Ontario, Canada

^h Vector Institute for Artificial Intelligence, Toronto, Ontario, Canada

ⁱ Li Ka Shing Knowledge Institute, St Michael's Hospital, Toronto, Ontario, Canada

^j Division of Neurosurgery, Krembil Neuroscience Centre, Toronto Western Hospital, University Health Network, Toronto, Ontario, Canada

ARTICLE INFO

Keywords:

Trigeminal neuralgia
Chronic neuropathic pain
Machine learning
Pain relief
Brain morphology

ABSTRACT

Background: Trigeminal neuralgia, a severe chronic neuropathic pain disorder, is widely believed to be amenable to surgical treatments. Nearly 20% of patients, however, do not have adequate pain relief after surgery. Objective tools for personalized pre-treatment prognostication of pain relief following surgical interventions can minimize unnecessary surgeries and thus are of substantial benefit for patients and clinicians.

Purpose: To determine if pre-treatment regional brain morphology-based machine learning models can prognosticate 1 year response to Gamma Knife radiosurgery for trigeminal neuralgia.

Methods: We used a data-driven approach that combined retrospective structural neuroimaging data and support vector machine-based machine learning to produce robust multivariate prediction models of pain relief following Gamma Knife radiosurgery for trigeminal neuralgia. Surgical response was defined as $\geq 75\%$ pain relief 1 year post-treatment. We created two prediction models using pre-treatment regional brain gray matter morphology (cortical thickness or surface area) to distinguish responders from non-responders to radiosurgery. Feature selection was performed through sequential backwards selection algorithm. Model out-of-sample generalizability was estimated via stratified 10-fold cross-validation procedure and permutation testing.

Results: In 51 trigeminal neuralgia patients (35 responders, 16 non-responders), machine learning models based on pre-treatment regional brain gray matter morphology (14 regional surface areas or 13 regional cortical thicknesses) provided robust *a priori* prediction of surgical response. Cross-validation revealed the regional surface area model was 96.7% accurate, 100.0% sensitive, and 89.1% specific while the regional cortical thickness model was 90.5% accurate, 93.5% sensitive, and 83.7% specific. Permutation testing revealed that both models performed beyond pure chance ($p < 0.001$). The best predictor for regional surface area model and regional cortical thickness model was contralateral superior frontal gyrus and contralateral isthmus cingulate gyrus, respectively.

Conclusions: Our findings support the use of machine learning techniques in subsequent investigations of chronic neuropathic pain. Furthermore, our multivariate framework provides foundation for future development of generalizable, artificial intelligence-driven tools for chronic neuropathic pain treatments.

Abbreviations: ML, machine learning; SBS, sequential backward selection; SVM, support vector machine.

* Corresponding author at: Toronto Western Hospital, Division of Neurosurgery, 399 Bathurst Street, 4W W-443, Toronto, Ontario M5T 2S8, Canada.

E-mail address: mojgan.hodaie@uhn.ca (M. Hodaie).

<https://doi.org/10.1016/j.nicl.2021.102706>

Received 2 January 2021; Received in revised form 19 May 2021; Accepted 20 May 2021

Available online 25 May 2021

2213-1582/© 2021 Published by Elsevier Inc. This is an open access article under the CC BY-NC-ND license (<http://creativecommons.org/licenses/by-nc-nd/4.0/>).

1. Introduction

Approximately 6–8% of the population suffers from chronic neuropathic pain (Smith and Torrance, 2012), with a staggering impact on society and consumption of healthcare resources (Schaefer et al., 2014). Chronic pain can be accompanied by increasing complications/side effects arising from over-reliance on medications and unsuccessful surgical procedures. Personalized tools for the prediction of pain relief would provide significant benefit when considering surgical treatment. Trigeminal neuralgia is the most frequently occurring orofacial chronic neuropathic pain (Koopman et al., 2009). Recent studies using advanced imaging technology have revealed trigeminal nerve and brain-level neural abnormalities in trigeminal neuralgia (Desouza et al., 2013; DeSouza et al., 2014; Zhong et al., 2018) within central nervous system regions important for the sensory and affective processing of pain. While surgical treatment can be highly effective, approximately 20–30% of patients do not achieve significant pain relief and require multiple, repeated interventions (Hodaie and Coello, 2013).

Prior work using advanced brain imaging has pinpointed microstructural differences between responders and non-responders (DeSouza et al., 2015; Hung et al., 2019, 2017; Tohyama et al., 2019). For instance, assessment of diffusivity metrics pointed to non-responders having microstructural neural abnormalities located more centrally within the neuroaxis which are predictive of treatment outcome (e.g. axial and radial diffusivity abnormalities within the trigeminal nerve pontine segment) (Hung et al., 2017). Construction of accurate pre-treatment prognostication tools—potentially utilizing biomarkers specific to non-responders—can capture brain imaging differences and potentially predict treatment outcome. In this study, using machine learning (ML) models, we aimed to investigate if pre-treatment regional brain gray matter morphology (regional cortical thickness or regional surface area) can serve as effective pre-treatment predictors of 1 year response to surgical intervention for trigeminal neuralgia. We hypothesized that these brain-based models will exhibit superior prognostication abilities than prior nerve-based models (Hung et al., 2017; Tohyama et al., 2019).

2. Methods

2.1. Patient recruitment

51 patients with trigeminal neuralgia defined by the International Classification of Headache Disorders 3rd Edition (International Headache Society, 2018) recruited locally at our surgical center were included in this study. Sample size for ML study of chronic pain is generally set by precedent. In this regard, our sample size of 51 is comparable to the literature (Lee et al., 2019; López-Solà et al., 2017; Zhong et al., 2018). All patients were medically refractive and treated with Gamma Knife radiosurgery as their first surgical treatment for unilateral trigeminal neuralgia. Restricting our study to one surgery helps minimize confounding effects from having multiple types of interventions on prognostication of treatment outcome. Research study approval in accordance with the Declaration of Helsinki was obtained from our institutional research ethics board with informed patient consent waived for retrospective cross-sectional brain imaging studies.

2.2. Automated regional surface area and regional cortical thickness extractions

We used a 3 Tesla GE Signa HDx magnetic resonance imaging scanner (General Electric Healthcare, Milwaukee) with an 8-channel head coil to acquire anatomical T1-weighted images from all patients (fast-spoiled gradient echo, TE = 5.1 ms, TR = 12.0 ms, flip angle = 20°, voxel size = 0.86 mm × 0.86 mm × 1.00 mm, 256 × 256 matrix, field of view = 22 cm, 146 slices). Between 2008 and 2017, we collected a single, pre-treatment T1-weighted image for each patient. FreeSurfer

(version 6.0, <http://surfer.nmr.mgh.harvard.edu>), was then used to automatically extract pre-treatment regional surface area and regional cortical thickness measurements from all 68 brain regions defined in the Desikan-Killiany atlas (Desikan et al., 2006). In this study, we extracted regional surface area and regional cortical thickness according to FreeSurfer's definitions. Regional surface area is calculated along the brain gray matter/white matter interface while regional cortical thickness is calculated as the distance between gray matter/white matter interface and gray matter/cerebrospinal fluid interface. Following extraction, all gray matter measures were standardized to unit variance and labeled with respect to pain laterality (ipsilateral or contralateral) to facilitate subsequent ML analyses. Quality checks were conducted to ensure there were no missing data from FreeSurfer automatic extractions. All subjects were successfully processed.

2.3. Surgical treatment for pain and treatment response grouping

We performed Gamma Knife radiosurgery to treat trigeminal neuralgia pain using either Elekta 4C© or Elekta Perfexion© systems (Elekta, Stockholm, Sweden) and 4 mm collimators. For all patients, according to best practices, a single 80 Gy radiation isodose was delivered to the cisternal segment of the symptomatic trigeminal nerve. To minimize adverse effects, brainstem radiation was constricted to 15 Gy to 1 mm³. Based on prior publications (DeSouza et al., 2015; Li et al., 2004; Tohyama et al., 2019), responder status was determined on a 75% threshold set at 1-year post-treatment compared to pre-treatment levels with responders exhibiting ≥ 75% pain intensity reduction and non-responders demonstrating < 75% pain intensity reduction. All pain intensity measurements were conducted on a 11-points numerical rating scale (from 0 denoting complete absence of pain to 10 defined as the worst pain imaginable) (Hawker et al., 2011).

2.4. Machine learning

We constructed two separate families of ML prediction models—one involving 68 pre-treatment regional surface areas and the other involving 68 pre-treatment regional cortical thicknesses as input features. Separate families of ML models were constructed as regional surface area and regional cortical thickness are mathematically orthogonal to each other and can provide independent insights into morphological changes in the brain. More specifically, regional surface area is measured on a single brain interface while regional cortical thickness is measured as the average distance between two non-overlapping brain interfaces. We implemented all ML models using Scikit-learn (0.20.1, <http://scikit-learn.org/stable/index.html>)—a Python library for ML. We chose support vector machine (SVM) as the ML technique for this study as SVM does not require extensive computational resources to determine the hyperplane that best separates an outcome variable within a multi-dimensional space. A linear kernel was used for all SVM models with the following hyperparameters (C = 1, gamma = 1/number of features, tolerance = 0.001). For dimensionality reduction, we used the sequential backward selection (SBS) procedure implemented in Mlxtend (0.17.0, <http://rasbt.github.io/mlxtend>) which can effectively eliminate features not useful for prediction of the outcome variable to arrive at improved prediction accuracies. To ensure our ML models are generalizable, we obtained estimates of out-of-sample model accuracy, sensitivity, and specificity using a stratified 10-fold cross-validation procedure which has been shown to be useful for ML problems with potentially imbalanced outcome classes. We selected stratified 10-fold cross-validation as it has been shown to be more reliable than other cross-validation procedures such as leave-one-out which can lead to overly variable estimates of ML model performance (Varoquaux et al., 2017).

Our ML framework included SVM and SBS over five steps to arrive at an optimal SVM model for each family (Fig. 1). First, we constructed a baseline SVM model using the complete set of 71 input features

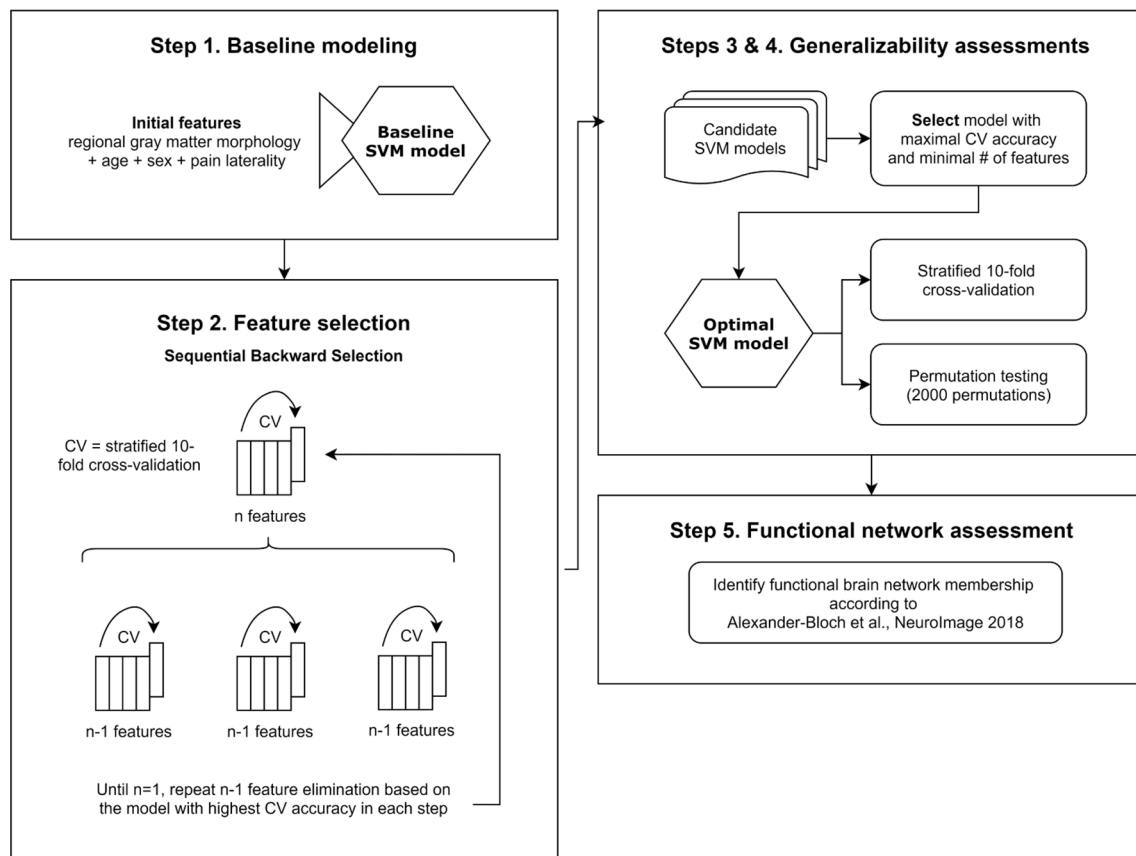


Fig. 1. Brain morphology-driven machine learning framework to predict 1 year response to treatment for chronic neuropathic pain. Machine learning techniques were used to create multivariate models capable of predicting 1 year response to surgery for individuals with trigeminal neuralgia. An initial model was first constructed from either cortical thickness or surface area features along with patient age, sex, and pain laterality. A collection of candidate support vector machine (SVM) models was then constructed using sequential backward selection for feature selection. To address the potential issue of model overfitting, model generalizability (accuracy, sensitivity, and specificity) were assessed via stratified 10-fold cross-validation and permutation testing. Our framework ultimately identified the SVM model with the highest cross-validated accuracy and lowest number of features/predictors as the optimal model. To better understand the functional relevance of the predictors included in the optimal model, we then consulted Alexander-Bloch et al.'s work which related Desikan-Killiany structural brain atlas with Yeo 7 functional brain network.

including 68 regional brain gray matter morphological measures (regional surface areas or regional cortical thicknesses), age, sex, and pain laterality. Second, we applied the SBS procedure to create a collection of candidate SVM models. Third, from SBS-generated collection of candidate SVM models, we identified the optimal SVM model which had maximal stratified 10-fold cross-validated prediction accuracy and minimal number of input features. Fourth, we used permutation testing (2000 permutations) to ensure that the optimal model performed at a prediction accuracy beyond pure chance ($p < 0.05$). Finally, we consulted the spatial correspondence recently reported by Alexander-Bloch et al. (Alexander-Bloch et al., 2018) between Desikan-Killiany structural brain atlas (Desikan et al., 2006) and Yeo 7 functional brain network atlas (Yeo et al., 2011) to identify which functional brain network each feature/predictor belonged to.

2.5. Post-hoc Bonferroni corrected Student's t-tests

Multiple post-hoc Bonferroni corrected Student's t-tests were conducted between trigeminal neuralgia patients against sex- and age-matched healthy controls to characterize the directionalities of regional gray matter morphology alterations contributing to each optimal treatment response model. These comparisons were conducted against 51 age- and sex-matched healthy control subjects without known history or diagnosis of neuropsychiatric and pain disorders from the Cam-CAN database (Taylor et al., 2017). For the regional surface area model, Bonferroni correction was conducted for 28 simultaneous

comparisons (14 features by 2 pain laterality) while for the regional cortical thickness model, Bonferroni correction was conducted for 26 simultaneous comparisons (13 features by 2 pain laterality).

2.6. Data availability statement

Anonymized data and code supporting study findings is available from the corresponding author upon reasonable request. Machine learning framework code is available on GitHub (<https://github.com/hungs/GMSxPredict>).

3. Results

3.1. Patient demographics

Of the 51 patients included in the study, all were diagnosed with trigeminal neuralgia (33 females, 18 males). 21 patients exhibited left-sided pain while 30 patients exhibited right-sided pain. Mean patient age at the time of treatment was 62.1 ± 13.6 standard deviation years. Pre-treatment pain intensity was reported on average at 9.0 ± 1.5 standard deviation out of 10 points. The mean pain intensity was reduced to 2.2 ± 3.4 standard deviation out of 10 points one year after Gamma Knife radiosurgery. On an individual patient basis, using a response criterion of $\geq 75\%$ post-treatment pain reduction, 35 of 51 patients were classified as responders while the remaining 16 were classified as non-responders. For more information, please refer to

detailed patient demographics in Table 1. Additional pain characteristics are detailed in Supplemental table 1. Age and sex of matched healthy controls can be found in Supplemental table 2.

3.2. Regional surface area model was highly predictive of 1 year pain relief

The regional surface area model predicted responders from non-responders with a statistically significant, cross-validated, testing accuracy of 96.7% (49.30/51.00) (Fig. 2). In addition, the model also achieved a cross-validated sensitivity of 100.0% (35.36/35.36) and cross-validated specificity of 89.1% (13.94/15.64). The area under the cross-validated receiver operating characteristic curve for this model was 0.97 ± 0.11 . This model identified regional surface areas from 14 brain regions spanning both hemispheres as relevant predictors of treatment response. Patient age, sex, and pain laterality were found to be irrelevant to treatment response. Regional surface area from the default

mode network, especially the contralateral superior frontal gyrus, appeared to be the best predictor of 1 year response to surgery for trigeminal neuralgia (Fig. 3). The remaining predictors in this model included: bilateral regional surface areas from pars triangularis and superior temporal gyrus; ipsilateral regional surface areas from entorhinal cortex, precentral gyrus, caudal middle frontal gyrus, pericalcarine cortex, paracentral lobule, superior parietal gyrus, and parahippocampal gyrus; and contralateral regional surface areas from caudal anterior cingulate gyrus and fusiform gyrus. Post-hoc group-level Bonferroni-corrected Student's t statistics revealed that these predictors remained at levels comparable with healthy control levels.

3.3. Regional cortical thickness model was highly predictive of 1 year pain relief

The regional cortical thickness model prognosticated responders from non-responders at a statistically significant, cross-validated, testing

Table 1
Detailed subject demographics.

ID	Sex	Age	Pain laterality	Branch	Pre-treatment pain intensity	Post-treatment pain intensity	Group	Pain dura.
P01	F	39	Left	V2, V3	5.5	0	Res	7
P02	F	46	Right	V1, V2, V3	10	0	Res	4
P03	F	47	Right	V1, V2, V3	10	0	Res	4
P04	F	49	Right	V1, V2	10	0	Res	5
P05	F	49	Left	V1, V2, V3	10	0	Res	3
P06	F	54	Left	V3	10	0	Res	8
P07	F	56	Right	V3	10	0	Res	23
P08	F	58	Right	V1, V2, V3	10	0	Res	3
P09	F	60	Right	V2, V3	7.5	1	Res	1.5
P10	F	62	Left	V2, V3	10	0	Res	10
P11	F	65	Right	V2	10	0	Res	30
P12	F	66	Left	V3	10	0	Res	7
P13	F	67	Left	V3	10	0	Res	3
P14	F	71	Left	V2, V3	10	0	Res	6
P15	F	74	Right	V2, V3	7	0	Res	8
P16	F	75	Right	V3	9.5	0	Res	2.5
P17	F	75	Right	V2, V3	8.5	0	Res	2
P18	F	79	Right	V2	10	0	Res	3
P19	F	79	Right	V3	10	0	Res	20
P20	F	80	Right	V3	7.5	0	Res	3
P21	F	83	Left	V1	10	0	Res	9
P22	F	86	Right	V3	8	0	Res	2
P23	M	32	Left	V1, V2	10	0	Res	2
P24	M	38	Right	V2, V3	10	0	Res	1.5
P25	M	41	Right	V1, V2	10	0	Res	2.5
P26	M	43	Left	V2	10	2	Res	1
P27	M	59	Right	V1, V2	10	0	Res	12
P28	M	59	Right	V3	10	0	Res	3
P29	M	62	Right	V2, V3	10	0	Res	9
P30	M	64	Right	V3	7	0	Res	2
P31	M	66	Left	V3	9.5	0	Res	5
P32	M	72	Right	V2, V3	10	1.75	Res	12
P33	M	79	Left	V2, V3	10	0	Res	10
P34	M	85	Left	V1, V2	8	0	Res	20
P35	M	86	Left	V2	8.5	0	Res	29
P36	F	36	Left	V2, V3	7.5	10	NRes	5
P37	F	45	Right	V1, V2	10	10	NRes	4
P38	F	47	Right	V1, V2, V3	10	3	NRes	3
P39	F	56	Left	V1, V2	6.5	7.75	NRes	3
P40	F	59	Right	V2, V3	9.5	2.5	NRes	2
P41	F	60	Right	V3	8	7	NRes	19
P42	F	63	Left	V2, V3	10	8	NRes	25
P43	F	65	Right	V3	10	8	NRes	1
P44	F	66	Right	V2, V3	10	3.5	NRes	10
P45	F	69	Left	V2, V3	9.5	4.5	NRes	8
P46	F	73	Right	V2, V3	10	6	NRes	31
P47	M	59	Right	V2	10	7	NRes	3
P48	M	62	Right	V1, V2, V3	8	8	NRes	20
P49	M	65	Left	V3	8	8	NRes	4
P50	M	67	Left	V1, V2	8	6	NRes	6
P51	M	67	Left	V2, V3	7.5	10	NRes	7

Abbreviations: L = Left, R = Right, V1 = ophthalmic branch of the trigeminal nerve, V2 = maxillary branch of the trigeminal nerve, V3 = mandibular branch of the trigeminal nerve, Res = responder, NRes = non-responder, Pain dura. = pain duration in years.

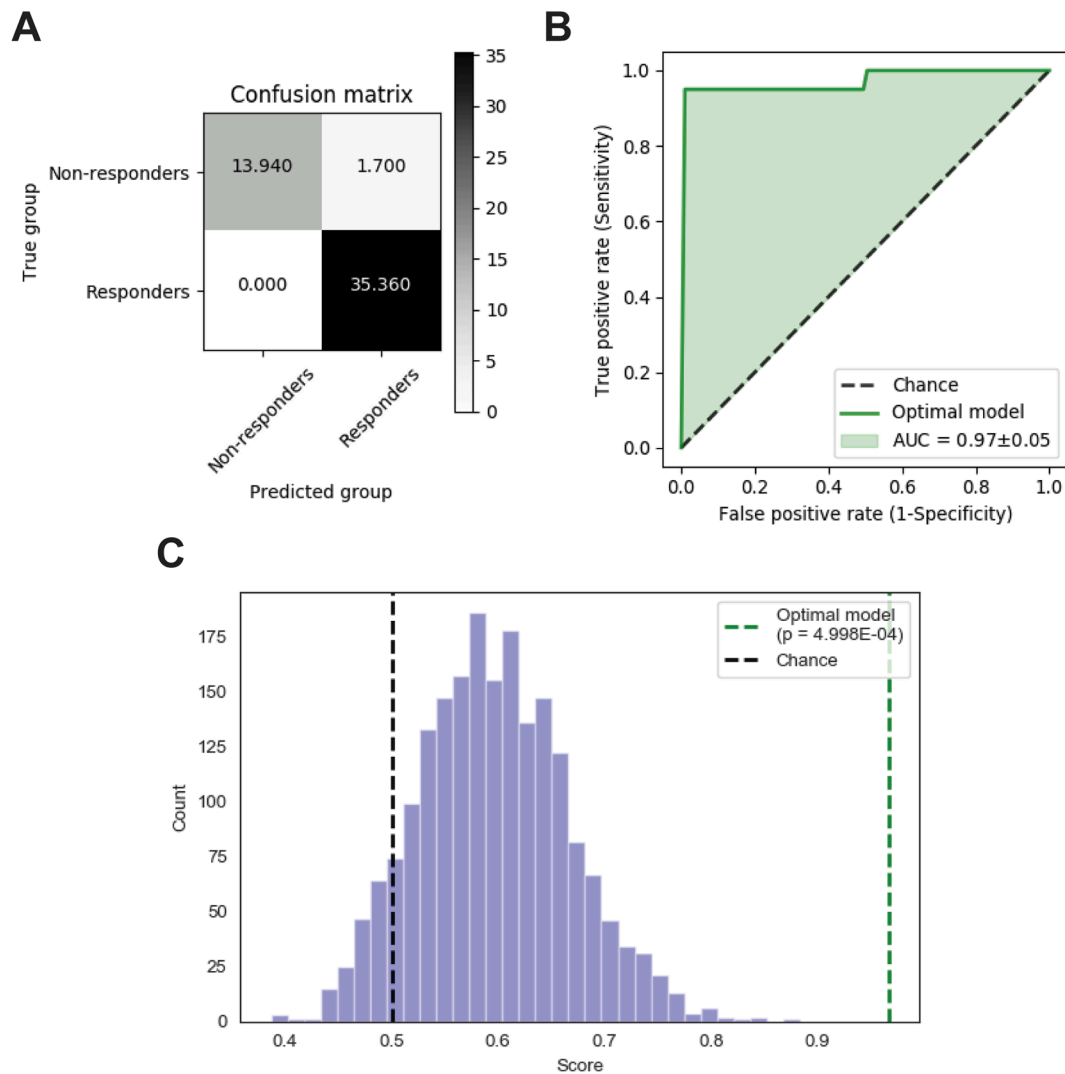


Fig. 2. Cross-validated prediction performance of the regional surface area model. Using 14 features, the regional surface area model created here successfully predicted 1 year outcome to surgery for trigeminal neuralgia at a high, cross-validated accuracy of 96.7%. The cross-validated sensitivity and specificity were 100.0% and 89.1%, respectively. A: The confusion matrix for this model demonstrated comparable performance for both response groups. Scalar bar serves as a guide for the average number of individuals within each quadrant of the confusion matrix. B: Receiver operating characteristic curve for the model revealed a cross-validated area under curve (AUC) of 0.97 which suggests a high level of discriminative performance. C: Permutation testing indicated that the model performed at a prediction accuracy that is beyond chance (green line), $p < 0.001$. (For interpretation of the references to colour in this figure legend, the reader is referred to the web version of this article.)

accuracy of 90.5% (46.16/51.00) (Fig. 4). In addition, the model also achieved a cross-validated sensitivity of 93.5% (33.07/35.36) and cross-validated specificity of 83.7% (13.09/15.64). The area under the cross-validated receiver operating characteristic curve for this model was 0.96 ± 0.11 . This model leveraged upon 13 features which spanned both hemispheres. Patient age, sex, and pain laterality were found to be irrelevant to treatment response. Regional cortical thickness from the default mode network, specifically the contralateral isthmus cingulate gyrus, appeared to be the most effective predictor of 1 year response (Fig. 5). Additional predictors within the optimal regional cortical thickness model included: bilateral regional cortical thicknesses from lateral occipital gyrus and fusiform gyrus; ipsilateral regional cortical thicknesses from the whole insular cortex, superior parietal gyrus, pars triangularis, and inferior temporal gyrus; and contralateral regional cortical thicknesses from superior temporal gyrus, entorhinal cortex, lateral orbitofrontal gyrus, and pars orbitalis. Post-hoc group-level Bonferroni-corrected Student's t-statistics revealed that trigeminal neuralgia patients had significantly reduced regional cortical thickness compared to healthy controls within ipsilateral inferior temporal gyrus,

contralateral entorhinal cortex, contralateral lateral orbitofrontal gyrus, contralateral superior temporal gyrus, bilateral fusiform gyrus, and bilateral lateral occipital gyrus (see also Table 2).

4. Discussion

The evidence supporting the central nervous system's role in the modulation of trigeminal neuralgia pain has been increasingly recognized (Desouza et al., 2013; DeSouza et al., 2015, 2014; Vaculik et al., 2019; Zhong et al., 2018). In line with these observations, we demonstrated that central nervous system features, specifically pre-treatment regional brain gray matter morphology (14 regional surface areas or 13 regional cortical thicknesses) can provide robust *a priori* prediction of pain relief/surgical response in trigeminal neuralgia. Brain-based multivariate models appear to be highly predictive of 1 year pain relief, resulting in 96.7% and 90.5% cross-validated accuracies, respectively. This surpassed prior nerve-based prognostication models for trigeminal neuralgia pain relief ($>71.0\%$ accurate) (Hung et al., 2017; Tohyama et al., 2019). This is notable as the central nervous system

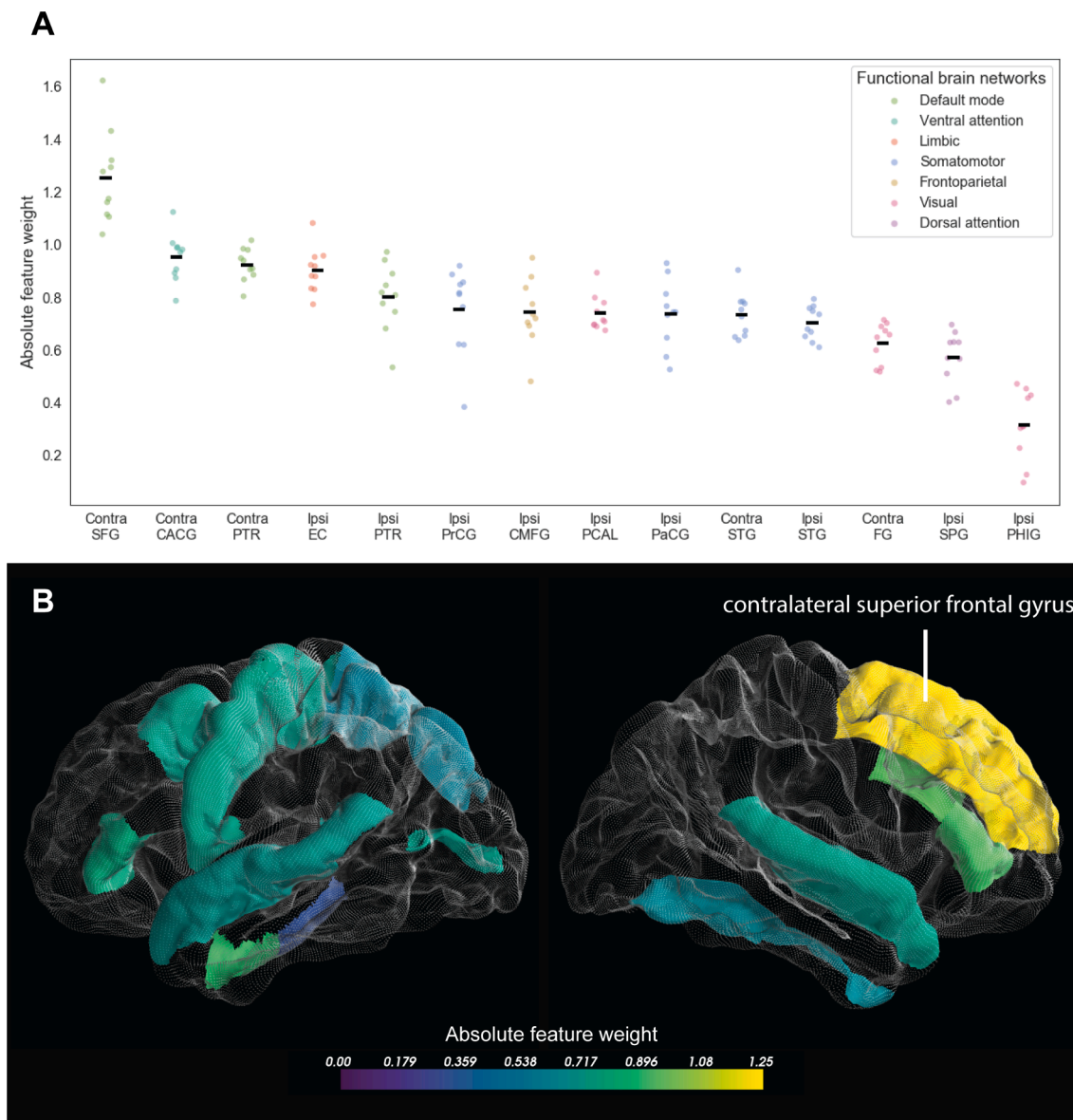


Fig. 3. Relative strengths of predictors in the regional surface area model. **A:** Regional surface area from the contralateral superior frontal gyrus is highly predictive of 1 year response to surgery in comparison to other features. Overall, the higher the mean feature weight, the more important a given feature is to the overall prediction accuracy. Black bars indicate mean absolute feature weight. Dots are within-fold feature weights. Contra = contralateral, Ipsi = ipsilateral, SFG = superior frontal gyrus, CACG = caudal anterior cingulate gyrus, PTR = pars triangularis, EC = entorhinal cortex, PrCG = precentral gyrus, CMFG = caudal middle frontal gyrus, PCAL = pericalcarine gyrus, PaCG = paracentral lobule, STG = superior temporal gyrus, FG = fusiform gyrus, SPG = superior parietal gyrus, PHIG = parahippocampal gyrus. **B:** This region is highlighted in the glass brain (left: ipsilateral brain, right: contralateral brain).

appears to be more accurate than the PNS at predicting response to surgical interventions for trigeminal neuralgia despite the pathogenesis of trigeminal neuralgia being strongly hypothesized to be associated with the peripheral nervous system. In other words, our study supports the central nervous system as a relatively stronger modulator of chronic neuropathic pain in trigeminal neuralgia than the peripheral nervous system.

4.1. Prior multivariate predictions of chronic neuropathic pain relief

Previous attempts at addressing treatment response, especially treatment response following surgical interventions for chronic neuropathic pain disorders such as trigeminal neuralgia, have centered largely around the utility of nerve-based biomarkers. In this realm, ML models were able to leverage microstructural information from trigeminal

nerves to pre-surgically predict 1 year pain relief at a moderate, cross-validated accuracy of 71.0% (Hung et al., 2017)—improving to 73.0% with early post-treatment data (Tohyama et al., 2019). Given the growing evidence that chronic neuropathic pain like trigeminal neuralgia is associated with gray and white matter alterations in brain regions important for affective and somatosensory dimensions of pain such as the insular cortices and somatosensory sensory cortices (Desouza et al., 2013; Obermann et al., 2013; Vaculik et al., 2019), we investigated multiple brain-based, regional gray matter morphological measures as pre-treatment predictors of surgical interventions for chronic neuropathic pain. Through this endeavour, we showed that ML models constructed from regional brain morphology such as regional surface area and regional cortical thickness are much more accurate than nerve-based models for the prognostication of 1 year surgical response in chronic neuropathic pain subjects. In particular, the regional surface

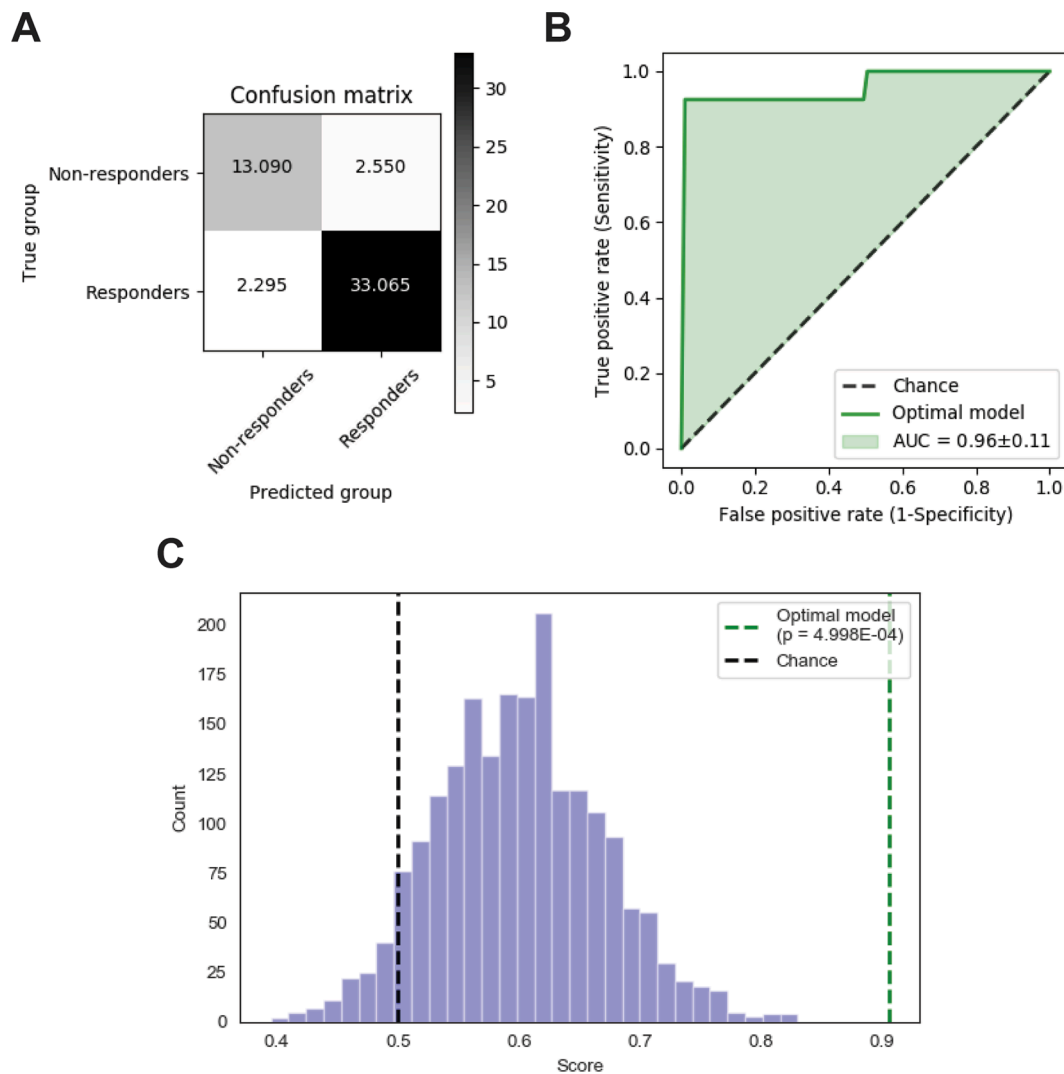


Fig. 4. Cross-validated prediction performance of the regional cortical thickness model. Using 13 features, the regional cortical thickness model successfully predicted 1 year outcome to surgery for trigeminal neuralgia at a cross-validated accuracy of 90.5%. The cross-validated sensitivity and specificity were 93.5% and 83.7%, respectively. Regional Cortical thickness model's accuracy, sensitivity, and specificity were lower than the regional surface area model. A: The confusion matrix for the cortical thickness model demonstrated comparable performance for both response groups. Scalar bar serves as a guide for the average number of individuals within each quadrant of the confusion matrix. B: Receiver operating characteristic curve for the regional cortical thickness model revealed a cross-validated area under curve (AUC) of 0.96 which suggests a high level of discriminative performance. C: Permutation testing indicated that the model performed at a prediction accuracy that is beyond chance (green line), $p < 0.001$. (For interpretation of the references to colour in this figure legend, the reader is referred to the web version of this article.)

area-based model achieved the highest accuracy (96.7%) which suggests that regional surface area differences, rather than regional cortical thickness differences, may more closely associate with surgical treatment response in chronic neuropathic pain.

4.2. Regional gray matter morphological underpinnings of chronic neuropathic pain

Prior literature on regional morphological alterations in brain gray matter in chronic neuropathic pain subjects have revealed widespread cortical thickness abnormalities. In comparison to healthy controls, subjects with orofacial chronic neuropathic pain showed thicker post-central gyrus, thinner insular cortex, and thinner cuneus cortex (Amaral et al., 2018; Hubbard et al., 2014; Maleki et al., 2015; Moayedi et al., 2011; Parise et al., 2014; Wang et al., 2017a, 2017b; Yang et al., 2017). Our current study adds to the clinical importance of these observations by showing insular cortical thickness is predictive of individual-level 1 year response to surgical interventions for orofacial chronic neuropathic

pain like trigeminal neuralgia. The literature on regional surface area alterations in chronic neuropathic pain, however, has been scarce (Wang et al., 2017a, 2017b). Here we observed that pre-treatment superior frontal gyrus surface area is highly predictive of 1 year treatment response after surgery for trigeminal neuralgia. As such, future studies are needed to better understand the role of regional surface area's involvement in various dimensions of orofacial chronic neuropathic pain and its relief. This potentially can be achieved via multivariate correlation analyses of regional surface areas with pain intensity, pain duration, and additional pain metrics.

4.3. The default mode network as a key hub of pain treatment response predictors

Chronic pain disorders are known to significantly alter resting state brain networks (Tsai et al., 2018; Wang et al., 2017a, 2017b; Zhang et al., 2018). In particular, the default mode network appears to be highly disrupted in trigeminal neuralgia whereby the cross-network

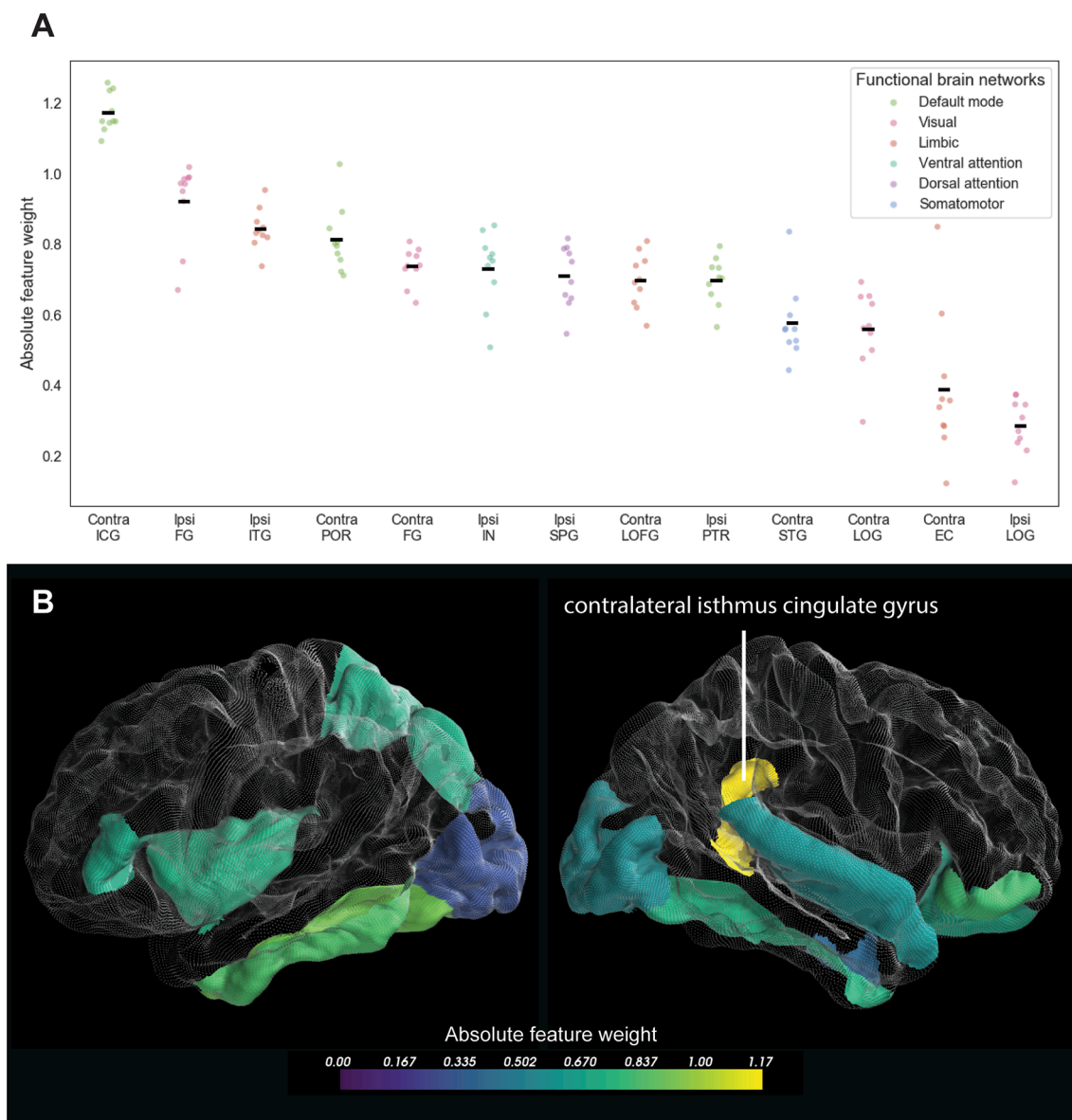


Fig. 5. Relative strengths of predictors in the regional cortical thickness model. A: Regional cortical thickness from contralateral isthmus cingulate gyrus is highly predictive of 1 year response to surgery in comparison to other features. Overall, the higher the mean feature weight, the more important a given feature is to the overall prediction accuracy. Black bars indicate mean absolute feature weight. Dots are within-fold feature weights. Contra = contralateral, Ipsi = ipsilateral, ICG = isthmus cingulate gyrus, FG = fusiform gyrus, ITG = inferior temporal gyrus, POR = pars orbitalis, FG = fusiform gyrus, IN = insular cortex, SPG = superior parietal gyrus, LOFG = lateral orbitofrontal gyrus, PTR = pars triangularis, STG = superior temporal gyrus, LOG = lateral occipital gyrus, EC = entorhinal cortex. B: This feature is further highlighted in the glass brain (left: ipsilateral brain, right: contralateral brain).

functional connectivity between default mode network to somatomotor/sensorimotor, frontoparietal, and limbic networks are markedly reduced (Tsai et al., 2018; Wang et al., 2017a, 2017b; Zhang et al., 2018). Our findings also reveal that the default mode network is a hub of regional gray matter morphological alterations that are superbly effective as predictors of 1 year response to surgical intervention for chronic neuropathic pain. Importantly, regional surface area from superior frontal gyrus and cortical thickness from isthmus cingulate cortex appeared to be the strongest predictors in this regard. Prior reports have associated a variety of plasticity changes—both functional and structural—within the superior frontal gyrus with trigeminal neuralgia pain duration and severity (Tsai et al., 2018; Xiang et al., 2019; Yuan et al., 2018). Conversely, the isthmus cingulate cortex, has been shown to exhibit focally accelerated gray matter loss with increasing age in humans (Grieve et al., 2011). It is therefore possible that varying degrees of default mode network regional gray matter alterations arising from

chronic pain, aging, and potential interactions between the two factors may differentiate trigeminal neuralgia surgery responders from non-responders.

4.4. Pain duration as a predictor of pain relief after Gamma Knife radiosurgery for trigeminal neuralgia

Patients with trigeminal neuralgia, especially those refractive to conventional pharmacological interventions, can experience prolonged pain duration often many years of pain. It is therefore important to perform exploratory analysis into the relative contribution of pain duration as a predictor of treatment outcome. When pain duration was included as a feature into our machine learning framework, the prediction accuracy increased by 2.5% and 3.3% for the regional cortical thickness model and regional surface area model, respectively. However, pain duration can be prone to recall bias and can therefore be

Table 2
Regional cortical thickness statistics contrasting TN patients and controls.

Region of interest	Pain laterality	t statistic	d.f.	p value	q value	Significance
Contralateral EC	Left	-4.06E + 00	4.31E + 01	2.05E-04	5.33E-03	**
Contralateral EC	Right	-3.61E + 00	3.60E + 01	9.26E-04	2.41E-02	*
Ipsilateral FG	Left	-5.18E + 00	6.59E + 01	2.31E-06	6.02E-05	***
Ipsilateral FG	Right	-3.72E + 00	3.70E + 01	6.61E-04	1.72E-02	*
Contralateral FG	Left	-5.18E + 00	6.59E + 01	2.31E-06	6.02E-05	***
Contralateral FG	Right	-3.72E + 00	3.70E + 01	6.61E-04	1.72E-02	*
Contralateral ICG	Left	2.40E-01	5.46E + 01	8.11E-01	1.00E + 00	n.s.
Contralateral ICG	Right	-8.93E-02	3.37E + 01	9.29E-01	1.00E + 00	n.s.
Ipsilateral IN	Left	-2.36E + 00	6.21E + 01	2.14E-02	5.55E-01	n.s.
Ipsilateral IN	Right	-1.26E + 00	3.88E + 01	2.14E-01	1.00E + 00	n.s.
Ipsilateral ITG	Left	-5.37E + 00	5.33E + 01	1.75E-06	4.55E-05	***
Ipsilateral ITG	Right	-3.55E + 00	3.30E + 01	1.17E-03	3.04E-02	*
Contralateral LOFG	Left	-4.61E + 00	6.32E + 01	2.00E-05	5.19E-04	***
Contralateral LOFG	Right	-3.85E + 00	2.88E + 01	6.02E-04	1.57E-02	*
Ipsilateral LOG	Left	-4.24E + 00	7.43E + 01	6.33E-05	1.65E-03	**
Ipsilateral LOG	Right	-3.98E + 00	3.52E + 01	3.33E-04	8.66E-03	**
Contralateral LOG	Left	-4.24E + 00	7.43E + 01	6.33E-05	1.65E-03	**
Contralateral LOG	Right	-3.98E + 00	3.52E + 01	3.33E-04	8.66E-03	**
Contralateral POR	Left	-7.19E-01	6.67E + 01	4.75E-01	1.00E + 00	n.s.
Contralateral POR	Right	-2.84E + 00	3.61E + 01	7.33E-03	1.91E-01	n.s.
Ipsilateral PTR	Left	-1.85E + 00	6.98E + 01	6.79E-02	1.00E + 00	n.s.
Ipsilateral PTR	Right	-8.20E-01	5.24E + 01	4.16E-01	1.00E + 00	n.s.
Ipsilateral SPG	Left	-2.52E + 00	7.77E + 01	1.39E-02	3.61E-01	n.s.
Ipsilateral SPG	Right	-1.63E + 00	6.14E + 01	1.08E-01	1.00E + 00	n.s.
Contralateral STG	Left	-5.42E + 00	5.41E + 01	1.41E-06	3.67E-05	***
Contralateral STG	Right	-5.24E + 00	4.82E + 01	3.48E-06	9.05E-05	***

Abbreviations: EC = entorhinal cortex, FG = fusiform gyrus, ICG = isthmus cingulate gyrus, ITG = inferior temporal gyrus, LOFG = lateral orbitofrontal gyrus, LOG = lateral occipital gyrus, POR = pars orbitalis, PTR = pars triangularis, SPG = superior parietal gyrus, STG = superior temporal gyrus, d.f. = degrees of freedom, q value = Bonferroni corrected p value, * = $q < 0.05$, ** = $q < 0.01$, *** = $q < 0.001$, n.s. = non-significant.

inaccurate. Given the limited increase in accuracy that pain duration provides, we believe future implementation studies should focus on the use of prediction models solely utilizing objective structural imaging features—bypassing the recall bias while maintaining a high level of treatment response (pain relief) prognostication performance.

5. Limitations

We note that our ML models are dependent on the availability of multivariate collections of morphological features. How individual features/predictors differentiate response groups apart remain to be explored in future studies with properly corrected group-level mass univariate statistics. Our study cohort are collected at a single surgical center. Despite this, our center receives broad patient referral across the nation, so the geographical selection bias is somewhat minimized. Through 10-fold stratified cross-validation we have obtained a reasonable estimate of out-of-sample generalizability at our institution. To further assess the out-of-institution generalizability, we recommend that future studies address the broader applicability and performance of our models at multiple international treatment centers for chronic neuropathic pain. This will also come with the additional benefit of being able to assess if our model is useful when provided with data from different MRI scanners. Both right-sided and left-sided trigeminal neuralgia pain patients were included in our study. We addressed this potential confound by including pain laterality in our ML framework. Sex and age of the patients were also included in our ML framework as these features are well-documented to impact chronic neuropathic pain. Our study cannot completely rule out possible involvement of pain medications (type and duration) on multivariate structural differentiation of radio-surgery response status and as such provides possible avenues for future pharmacological investigations. Despite this, our model performed at a high level without the information that these interactions may provide and arrived at sensible individual-level prediction of Gamma Knife radiosurgery treatment outcome for individuals with trigeminal neuralgia.

Conclusion: Towards brain-guided ML tools for chronic

neuropathic pain relief

Our current study, in conjunction with prior studies (Lee et al., 2019; Lindquist et al., 2017; López-Solà et al., 2017; Wager et al., 2013), supports the use of multivariate ML methods in future investigation and the development of individual-level clinical tools for chronic pain. Here, we developed an improved ML framework which addresses the common issue of overfitting in multidimensional, neuroimaging feature space. Our framework with the SBS procedure may serve as the crucial first step towards future ML studies on chronic pain populations and will likely lead to more generalizable, clinically useful, and translatable prognostication tools for chronic pain treatments. Given that our current brain-based models are constructed from readily available T1-weighted MRI data, they may be easily implemented clinically to further optimize surgical treatment selection for trigeminal neuralgia patients, mitigate the delivery of unnecessary treatments, and facilitate timely assessment for alternative pain treatments such as neuromodulation.

Acknowledgements

The authors would like to thank Hodaie lab clinical research database managers past and present for their contributions towards patient recruitment and database curation.

Funding

This study is supported by Canadian Institutes of Health Research Doctoral Research Award (Ref. # GSD157876) awarded to PSH, Canadian Institutes of Health Research Master's Research Award awarded to AN, Canadian Institutes of Health Research Doctoral Research Award (Ref. # GSD164127) awarded to ST, and Canadian Institutes of Health Research Operating Grant (Ref. # MOP130555) awarded to MH.

Competing interest statement

The authors declare no competing interests.

Appendix A. Supplementary data

Supplementary data to this article can be found online at <https://doi.org/10.1016/j.nicl.2021.102706>.

References

- Alexander-Bloch, A., Shou, H., Liu, S., Satterthwaite, T.D., Glahn, D.C., Shinohara, R.T., Vandekar, S.N., Raznahan, A., 2018. On testing for spatial correspondence between maps of human brain structure and function. *Neuroimage* 178, 540–551. <https://doi.org/10.1016/j.neuroimage.2018.05.070>.
- Amaral, V.C.G., Tukamoto, G., Kubo, T., Luiz, R.R., Gasparetto, E., Vincent, M.B., 2018. Migraine improvement correlates with posterior cingulate cortical thickness reduction. *Arq. Neuropsiquiatr.* 76, 150–157. <https://doi.org/10.1590/0004-282x20180004>.
- Desikan, R.S., Ségonne, F., Fischl, B., Quinn, B.T., Dickerson, B.C., Blacker, D., Buckner, R.L., Dale, A.M., Maguire, R.P., Hyman, B.T., Albert, M.S., Killiany, R.J., 2006. An automated labeling system for subdividing the human cerebral cortex on MRI scans into gyral based regions of interest. *Neuroimage* 31 (3), 968–980. <https://doi.org/10.1016/j.neuroimage.2006.01.021>.
- DeSouza, D.D., Moayed, M., Chen, D.Q., Davis, K.D., Hodaie, M., Binstok, A., 2013. Sensorimotor and pain modulation brain abnormalities in trigeminal neuralgia: a paroxysmal, sensory-triggered neuropathic pain. *PLoS One* 8 (6), e66340. <https://doi.org/10.1371/journal.pone.0066340>.
- DeSouza, D.D., Hodaie, M., Davis, K.D., 2014. Abnormal trigeminal nerve microstructure and brain white matter in idiopathic trigeminal neuralgia. *Pain* 155, 37–44. <https://doi.org/10.1016/j.pain.2013.08.029>.
- DeSouza, D.D., Davis, K.D., Hodaie, M., 2015. Reversal of insular and microstructural nerve abnormalities following effective surgical treatment for trigeminal neuralgia. *Pain* 156, 1112–1123. <https://doi.org/10.1097/j.pain.0000000000000156>.
- Grieve, S.M., Korgaonkar, M.S., Clark, C.R., Williams, L.M., 2011. Regional heterogeneity in limbic maturational changes: evidence from integrating cortical thickness, volumetric and diffusion tensor imaging measures. *Neuroimage* 55 (3), 868–879. <https://doi.org/10.1016/j.neuroimage.2010.12.087>.
- Hawker, G.A., Mian, S., Kendzerska, T., French, M., 2011. Measures of adult pain: Visual Analog Scale for Pain (VAS Pain), Numeric Rating Scale for Pain (NRS Pain), McGill Pain Questionnaire (MPQ), Short-Form McGill Pain Questionnaire (SF-MPQ), Chronic Pain Grade Scale (CPGS), Short Form-36 Bodily Pain Scale (SF-Arthritis Care Res. 63 (S11), S240–S252. <https://doi.org/10.1002/acr.v63.11s10.1002/acr.20543>.
- Hodaie, M., Coello, A.F., 2013. Advances in the management of trigeminal neuralgia. *J. Neurosurg. Sci.* 57, 13–21.
- Hubbard, C.S., Khan, S.A., Keaser, M.L., Mathur, V.A., Goyal, M., Seminowicz, D.A., 2014. Altered Brain Structure and Function Correlate with Disease Severity and Pain Catastrophizing in Migraine Patients. *eNeuro* 1. DOI:10.1523/ENEURO.0006-14.2014.
- Hung, P.-S.-P., Chen, D.Q., Davis, K.D., Zhong, J., Hodaie, M., 2017. Predicting pain relief: use of pre-surgical trigeminal nerve diffusion metrics in trigeminal neuralgia. *NeuroImage Clin.* 15, 710–718. <https://doi.org/10.1016/j.nicl.2017.06.017>.
- International Headache Society, 2018. The International Classification of Headache Disorders, 3rd edition. *Cephalalgia* 38, 1–211. DOI:10.1177/0333102417738202.
- Koopman, J.S.H.A., Dieleman, J.P., Huygen, F.J., de Mos, M., Martin, C.G.M., Sturkenboom, M.C.J.M., 2009. Incidence of facial pain in the general population. *Pain* 147, 122–127. <https://doi.org/10.1016/j.pain.2009.08.023>.
- Lee, J., Mawla, I., Kim, J., Loggia, M.L., Ortiz, A., Jung, C., Chan, S.-T., Gerber, J., Schmithorst, V.J., Edwards, R.R., Wasan, A.D., Berna, C., Kong, J., Kaptchuk, T.J., Gollub, R.L., Rosen, B.R., Napadow, V., 2019. Machine learning-based prediction of clinical pain using multimodal neuroimaging and autonomic metrics. *Pain* 160 (3), 550–560.
- Li, S.T., Pan, Q., Liu, N., Shen, F., Liu, Z., Guan, Y., Sindou, M., Burchiel, K.J., 2004. Trigeminal neuralgia: What are the important factors for good operative outcomes with microvascular decompression. *Surg. Neurol.* 62, 400–404. <https://doi.org/10.1016/j.surneu.2004.02.028>.
- Lindquist, M.A., Krishnan, A., López-Solà, M., Jelpma, M., Woo, C.-W., Koban, L., Roy, M., Atlas, L.Y., Schmidt, L., Chang, L.J., Reynolds Losin, E.A., Eisenbarth, H., Ashar, Y. K., Delk, E., Wager, T.D., 2017. Group-regularized individual prediction: theory and application to pain. *Neuroimage* 145, 274–287. <https://doi.org/10.1016/j.neuroimage.2015.10.074>.
- López-Solà, M., Woo, C.-W., Pujol, J., Deus, J., Harrison, B.J., Monfort, J., Wager, T.D., 2017. Towards a neurophysiological signature for fibromyalgia. *Pain* 158 (1), 34–47. <https://doi.org/10.1097/j.pain.0000000000000707>.
- Maleki, N., Barmettler, G., Moulton, E.A., Scrivani, S., Veggeberg, R., Spierings, E.L.H., Burstein, R., Becerra, L., Borsook, D., 2015. Female migraineurs show lack of insular thinning with age. *Pain* 156, 1232–1239. <https://doi.org/10.1097/j.pain.0000000000000159>.
- Moayed, M., Weissman-Fogel, I., Crawley, A.P., Goldberg, M.B., Freeman, B.V., Tenenbaum, H.C., Davis, K.D., 2011. Contribution of chronic pain and neuroticism to abnormal forebrain gray matter in patients with temporomandibular disorder. *Neuroimage* 55 (1), 277–286. <https://doi.org/10.1016/j.neuroimage.2010.12.013>.
- Obermann, M., Rodriguez-Raecke, R., Naegel, S., Holle, D., Mueller, D., Yoon, M.-S., Theysohn, N., Blex, S., Diener, H.-C., Katsarava, Z., 2013. Gray matter volume reduction reflects chronic pain in trigeminal neuralgia. *Neuroimage* 74, 352–358. <https://doi.org/10.1016/j.neuroimage.2013.02.029>.
- Parise, M., Kubo, T.T., Doring, T., Tukamoto, G., Vincent, M., Gasparetto, E., 2014. Cuneus and fusiform cortices thickness is reduced in trigeminal neuralgia. *J. Headache Pain* 15, 17. <https://doi.org/10.1186/1129-2377-15-17>.
- Schaefer, C., Sadosky, A., Mann, R., Daniel, S., Parsons, B., Tuchman, M., Ansel, A., Stacey, B.R., Nalamachu, S., Nieshoff, E., 2014. Pain severity and the economic burden of neuropathic pain in the United States: BEAT Neuropathic Pain Observational Study. *Clinicoecon. Outcomes Res.* 6, 483–496. <https://doi.org/10.2147/CEOR.S63323>.
- Hung, P.S.-P., Tohyama, S., Zhang, J.Y., Hodaie, M., 2019. Temporal disconnection between pain relief and trigeminal nerve microstructural changes after Gamma Knife radiosurgery for trigeminal neuralgia. *J. Neurosurg.* 1–9. DOI:10.3171/2019.4.JNS19380.
- Smith, B.H., Torrance, N., 2012. Epidemiology of neuropathic pain and its impact on quality of life. *Curr. Pain Headache Rep.* 16 (3), 191–198. <https://doi.org/10.1007/s11916-012-0256-0>.
- Taylor, J.R., Williams, N., Cusack, R., Auer, T., Shafto, M.A., Dixon, M., Tyler, L.K., Cam-CAN, Henson, R.N., 2017. The Cambridge Centre for Ageing and Neuroscience (Cam-CAN) data repository: Structural and functional MRI, MEG, and cognitive data from a cross-sectional adult lifespan sample. *Neuroimage* 144, 262–269. DOI:10.1016/j.neuroimage.2015.09.018.
- Thomas Yeo, B.T., Krienen, F.M., Sepulcre, J., Sabuncu, M.R., Lashkari, D., Hollinshead, M., Roffman, J.L., Smoller, J.W., Zöllei, L., Polimeni, J.R., Fischl, B., Liu, H., Buckner, R.L., 2011. The organization of the human cerebral cortex estimated by intrinsic functional connectivity. *J. Neurophysiol.* 106 (3), 1125–1165. <https://doi.org/10.1152/jn.00338.2011>.
- Tohyama, S., Hung, P.S.-P., Zhong, J., Hodaie, M., 2018. Early postsurgical diffusivity metrics for prognostication of long-term pain relief after Gamma Knife radiosurgery for trigeminal neuralgia. *J. Neurosurg.* 1–10. DOI:10.3171/2018.3.JNS172936.
- Tsai, Y., Yuan, R., Patel, D., Chandrasekaran, S., Weng, H., Yang, J., Lin, C., Biswal, B.B., 2018. Altered structure and functional connection in patients with classical trigeminal neuralgia. *Hum. Brain Mapp.* 39 (2), 609–621. <https://doi.org/10.1002/hbm.v39.210.1002/hbm.23696>.
- Vaculic, M.F., Noorani, A., Hung, P.-P., Hodaie, M., 2019. Selective hippocampal subfield volume reductions in classic trigeminal neuralgia. *NeuroImage Clin.* 23, 101911. <https://doi.org/10.1016/j.nicl.2019.101911>.
- Varoquaux, G., Raamana, P.R., Engemann, D.A., Hoyos-Idrobo, A., Schwartz, Y., Thirion, B., 2017. Assessing and tuning brain decoders: cross-validation, caveats, and guidelines. *Neuroimage* 145, 166–179. <https://doi.org/10.1016/j.neuroimage.2016.10.038>.
- Wager, T.D., Atlas, L.Y., Lindquist, M.A., Roy, M., Woo, C.-W., Kross, E., 2013. An fMRI-based neurologic signature of physical pain. *N. Engl. J. Med.* 368 (15), 1388–1397. <https://doi.org/10.1056/NEJMoa1204471>.
- Wang, Y., Cao, D.-yuan., Remeniuk, B., Krimmel, S., Seminowicz, D.A., Zhang, M., 2017a. Altered brain structure and function associated with sensory and affective components of classic trigeminal neuralgia. *Pain* 158 (8), 1561–1570. <https://doi.org/10.1097/j.pain.0000000000000951>.
- Wang, Y., Zhang, Y., Zhang, J., Wang, J., Xu, J., Li, J., Cui, G., Zhang, J., 2017b. Structural and Functional Abnormalities of the Insular Cortex in Trigeminal Neuralgia: A Multimodal MRI Analysis. *Pain*. <https://doi.org/10.1097/j.pain.0000000000001120>.
- Xiang, C.-Q., Liu, W.-F., Xu, Q.-H., Su, T., Yong-Qiang, S., Min, Y.-L., Yuan, Q., Zhu, P.-W., Liu, K.-C., Jiang, N., Ye, L., Shao, Y., 2019. Altered spontaneous brain activity in patients with classical trigeminal neuralgia using regional homogeneity: a resting-state functional MRI study. *Pain Pract.* 19, 397–406. <https://doi.org/10.1111/papr.12753>.
- Yang, Q., Wang, Z., Yang, L., Xu, Y., Chen, L.M., 2017. Cortical thickness and functional connectivity abnormality in chronic headache and low back pain patients. *Hum. Brain Mapp.* 38 (4), 1815–1832. <https://doi.org/10.1002/hbm.23484>.
- Yuan, J., Cao, S., Huang, Y., Zhang, Y., Xie, P., Zhang, Y., Fu, B., Zhang, T., Song, G., Yu, T., Zhang, M., 2018. Altered spontaneous brain activity in patients with idiopathic trigeminal neuralgia: a resting-state functional MRI study. *Clin. J. Pain* 34, 600–609. <https://doi.org/10.1097/AJP.0000000000000578>.
- Zhang, Y., Mao, Z., Pan, L., Ling, Z., Liu, X., Zhang, J., Yu, X., 2018. Dysregulation of pain- and emotion-related networks in trigeminal neuralgia. *Front. Hum. Neurosci.* 12, 1–10. <https://doi.org/10.3389/fnhum.2018.00107>.
- Zhong, J., Chen, D.Q., Hung, P.-P., Hayes, D.J., Liang, K.E., Davis, K.D., Hodaie, M., 2018. Multivariate pattern classification of brain white matter connectivity predicts classic trigeminal neuralgia. *Pain* 159 (10), 2076–2087. <https://doi.org/10.1097/j.pain.0000000000001312>.